ORIGINAL ARTICLE

Effect of CFRP anchorages on the flexural behavior of externally strengthened reinforced concrete beams

Jamal A. Abdalla[1] · Alnadher B. Ali[2] · Rami A. Hawileh[1] · Haya H. Mhanna[1] · Khalid E. Galal[3] · Elias I. Saqan[4]

Abstract

Advanced composite materials in the form of fiber-reinforced polymer (FRP) have been gaining popularity in the construction industry. One of the main challenges of using externally bonded FRP in repair and strengthening applications is its susceptibility to peeling-off or delamination without achieving the full capacity of the FRP material. Anchoring the FRP laminates has been deemed effective in delaying debonding failure, thus ensuring load continuity between the concrete and FRP. This paper aims to study the effect of two anchorage systems on the strength and ductility of reinforced concrete (RC) beams strengthened with carbon FRP (CFRP) laminates. The anchors considered in this study were end U-wraps and CFRP spike anchors. A total of seven RC beams were cast and strengthened with different arrangements of CFRP laminates and anchors. The test parameters investigated in this study include the length of the FRP sheet, type of anchor, and the number of CFRP spike anchors. Test results showed that flexural strengthening using CFRP laminates enhanced the capacity of the unstrengthened beam by 16–41% at the expense of ductility. Using full-length CFRP sheets significantly improved the overall performance of the beams as opposed to short-length CFRP sheets. Out of the anchored specimens, the best improvement in the capacity was achieved in the specimen anchored with end U-wraps. CFRP spike anchors provided limited enhancement in the load-carrying capacity of the specimens. The efficiency of the spike anchors could be upgraded if longer embedment depth and larger dowel diameter were used. Finally, the ACI440.2R-17 strength predictions were in good agreement with the experimental results.

Keywords Carbon fiber-reinforced polymers · Reinforced concrete · Flexural strengthening · U-wraps · FRP spike anchors

1 Introduction

Aging and deterioration of the infrastructure is a major challenge in the civil engineering industry. Factors such as design or construction errors, corrosion of the embedded reinforcement, changes in the structure usage, and seismic retrofit have made strengthening existing reinforced concrete (RC) structures essential [1–4]. Within the past few decades, new technology has emerged using fiber-reinforced polymers (FRPs) to refurbish and retrofit RC structures. The advantageous basic properties of these materials, including high strength-to-weight ratios, non-corrosiveness, and electro-magnetic neutrality, have made FRP composites suitable materials for strengthening and rehabilitation of RC structures [5–8]. In addition, the continuous reduction in its cost due to mass production resulted in making FRP-based strengthening and rehabilitation techniques economically competitive.

Externally bonded FRP sheets/laminates have been successfully utilized to enhance the flexural and/or shear capacity of RC beams [9–12], provide confinement to RC columns [13, 14], and strengthen walls subjected to out-of-plane and in-plane loading [15, 16]. However, the effectiveness of the FRP retrofitting technique depends mainly on the stress transfer performance and the strength of the FRP–concrete

✉ Elias I. Saqan
elias.saqan@austin.utexas.edu

1 Department of Civil Engineering, American University of Sharjah, Sharjah, United Arab Emirates

2 American University of Sharjah, Sharjah, United Arab Emirates

3 Department of Building, Civil and Environmental Engineering, Concordia University, Montréal, Québec, Canada

4 Maseeh Department of Civil, Architectural and Environmental Engineering, The University of Texas at Austin, Austin, TX, USA

interface. Early failure at the interface typically causes delamination at the epoxy–concrete interface or debonding at the epoxy–FRP interface. In both cases, the FRP becomes ineffective once it separates from the concrete [17–20].

To improve the performance of FRP strengthened members, recent studies have addressed numerous ways to mitigate or prevent debonding failure, out of which anchoring the laminates have shown promising results [21–26]. The primary role of the anchors is to provide load continuity between the FRP and concrete after local debonding [11]. This could be accomplished either by providing confinement to the laminates, such as U-wraps, or by redistributing shear stresses at the bond interface, such as mechanical anchors or FRP spike anchors.

Although a notable amount of experimental research has been conducted to examine the effect of different anchorage systems on the flexural capacity of FRP strengthened members [27–31], guidelines and models for the effective strain of anchored FRP laminates were not fully defined in the literature. Accordingly, extensive testing is still needed to examine the effect of several parameters on the performance of externally strengthened beams with anchors. A study by Valivonis et al. [28] showed that the capacity enhancement due to strengthening depended mainly on the anchorage system. Anchoring the laminates with carbon FRP (CFRP) hoops at the end of the flexural CFRP sheets provided better flexural capacity enhancement than the unanchored strengthened specimen and the specimen anchored with cotters by 40% and 35%, respectively. Overall, the efficiency of the anchors was evident only after the yielding stress of the internal steel reinforcement was attained [28]. In a recent study by Zhang et al. [32], the authors studied the effect of the U-wrap spacing, FRP reinforcement ratio, and concrete compressive strength on the flexural capacity of RC T-beam specimens. Experimental results study showed that increasing the flexural reinforcement ratio from 0.95 to 1.29% led to a 48% enhancement in the ultimate load. On the other hand, the concrete compressive strength and U-wrap spacing had a marginal influence on the strength resistance. Nonetheless, reducing the U-wrap spacing increased the stiffness of the beam, which delayed the cracking of the concrete [32].

Similarly, a series of experimental investigations were conducted to test the effectiveness of FRP spike anchors [33–39]. In a study by Zaki et al. [40], the authors examined flexural strengthening of RC T-beams using CFRP laminates and different configurations of CFRP spike anchors. The experimental results showed that increasing the fiber content in the anchors caused better enhancement in the capacity. In addition, more and closely spaced anchors performed better than fewer and further apart anchors [40]. In another study by Kim et al. [41], the authors tested ten RC beams to investigate the effectiveness of CFRP spike anchors and U-wrap anchors. Test results showed that U-wraps performed inferior to the CFRP spike anchors as the U-wraps did not provide a force component in the direction of the main CFRP sheet. The effect of the U-wraps was similar to the CFRP anchors only when one layer of flexural CFRP sheet was used. Overall, the best strength enhancement was provided when CFRP anchors were installed on the U-wraps and main CFRP sheet [41].

2 Research significance

The effectiveness of the FRP retrofitting technique is hindered by the early debonding failure of the FRP laminates, which limits the utilization of the FRP tensile strength. To prevent or rather delay debonding, an anchorage system comprising FRP U-wraps could be used to confine the flexural FRP reinforcement. Such a system works relatively well, provided that the surface of the concrete is undamaged and is able to transfer the resulting stresses. However, this method may not be feasible if the concrete surface is weathered and/or damaged, which results in an improper bond between the FRP and the concrete. Furthermore, the U-wraps cannot be implemented in wide structural elements, such as slabs. For the aforementioned reasons, it may be more appropriate to use FRP spike anchors that can be embedded inside the concrete. Despite the numerous research on FRP strengthening systems, accurate models for determining the capacity gained by anchoring FRP laminates in flexure are limited. In addition, the comparison between different anchorage systems such as U-wraps and various FRP spike anchors arrangements has rarely been conducted. This study addresses the research gap via testing seven RC beam specimens under four-point bending tests. The effect of influential test variables, including anchor type, FRP reinforcement ratio, length of the FRP sheet, and the number and configuration of FRP spike anchors, were discussed and analyzed. Based on the experimental results, recommendations for improving the developed and tested anchorage systems are proposed.

3 Experimental program

3.1 Test specimens

A total of seven RC beams were designed and cast in one batch using self-consolidating concrete (SCC). Each beam was 1840 mm long, 120 mm wide, and 240 mm deep, as shown in Fig. 1. The top/bottom and side covers were 25 and 15 mm, respectively. The beams were heavily reinforced in shear with φ8 mm stirrups spaced at 80 mm center-to-center to force flexural failure. The U-wraps, which are intended for anchoring the flexural CFRP, will further enhance the shear

Fig. 1 Beam reinforcement details. **a** Front view and **b** cross section

(a) Front view

(b) Cross-section
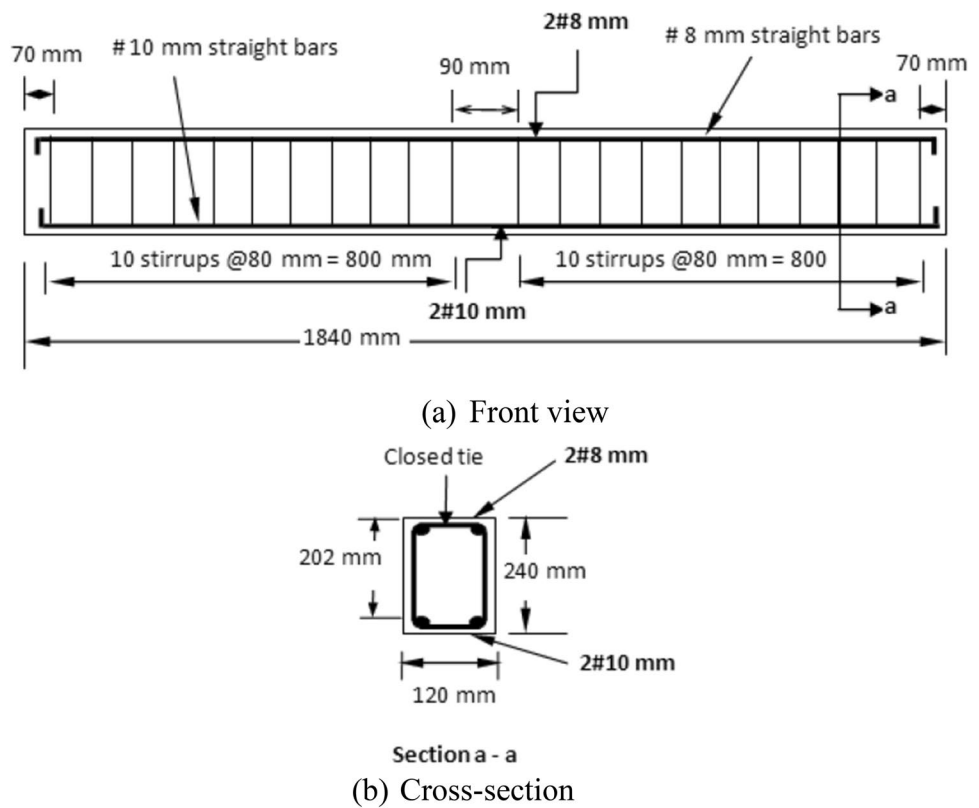
strength of the beams. However, they were not included in the shear design since not all beams have U-wraps. The bottom flexural reinforcement comprised two φ10 mm steel bars located at a depth of 202 mm from the extreme compression fiber of the beam, as shown in Fig. 1. In addition, two φ8 mm steel bars located at a depth of 38 mm were used to hold the stirrups.

3.2 Material properties

3.2.1 Concrete

All beam specimens were cast in a ready-mix plant with self-consolidating concrete (SCC). The concrete mix comprised ground granulated blast-furnace slag (GGBS), multiple chemical additives, super-plasticizer, and silica fume. The concrete had a w/c ratio of 0.36 and density of 2459 kg/m³. During casting, a total of sixteen 4×8 standard cylinders (height: 200 mm and diameter: 100 mm) were cast and cured under the same conditions as the test beams. All sixteen cylinders were tested at 28 days (testing week), eleven cylinders were tested under compression in accordance with ASTM C39/C39M-18 [42], and five cylinders were tested for tension strength using the split cylinder test in accordance with ASTM C496/C496M-11 [43]. In addition, twelve cubes were tested under compression in accordance with BS 1881–116: 1983 [44]: Four cubes were tested at 4 days of concrete casting, four cubes at 28 days, and four cubes at 56 days. The average results of the accepted samples of all tests are summarized in Table 1.

As shown in Table 1, the cylindrical concrete compressive strength (f'_c) was 44.6 MPa. The calculated tensile strength presented about 9.6% of f'_c. In addition, the cylindrical compressive strength was 58% of the cube strength.

Table 1 Concrete mechanical properties

Sample	Material property	Days	Average (MPa)	SD (MPa)	COV (%)
Cylinders	Compressive Strength (MPa)	28	44.6	1.7	3.7
	Tensile Strength (MPa)	28	4.3	0.6	13.0
Cubes	Compressive Strength (MPa)	4	59.9	3.3	5.5
		28	77.0	1.3	1.7
		56	79.5	4.0	5.0

SD standard deviation, *COV* coefficient of variance

Since all beams were tested between 28 and 56 days, and the increase in strength within this time period was only 3.2% (77 to 79.5 MPa), the 28-day strength values were used in the analysis. 3.2.2 Steel.

Three samples of 8 mm and 10 mm steel bars were tested under tension in a universal testing machine (UTM) to obtain the mechanical properties of the reinforcement bars. Test results in terms of average yield stress (f_y), strain at yield (ε_y), ultimate strength (f_u), and modulus of elasticity (E_s) are summarized in Table 2.

3.2.2 CFRP sheets and epoxy

Unidirectional carbon fiber fabric was used in this project to prepare the CFRP sheets and anchors (SikaWrap-300C [45]). The CFRP sheets and anchors were impregnated with Sikadur-330 [46] two-part epoxy adhesive. Table 3 shows the mechanical properties of the CFRP dry sheet, laminate, and epoxy adhesive as provided by the manufacturer.

3.3 Test matrix

Seven RC beams were tested to investigate different configurations of CFRP sheets and anchors simulating an FRP-strengthened structure. All specimens had similar CFRP width of 120 mm. The test parameters included the length of the CFRP reinforcement, the presence or absence of anchorage system, type of anchors, and the number of anchors. The test matrix is summarized in Table 4. Beam designations are explained as follows: CB: control beam, SB: strengthened beam, Sh: sheet, F: full-length, S: short-length, U: end U-wraps, A: CFRP spike anchors, and the number preceding A: number of anchors.

As shown in Table 4, two specimens have unanchored CFRP laminates to serve as control specimens for the anchored ones. One specimen was strengthened with

Table 4 Test matrix

Beam designation	Length of CFRP sheet (m)	Anchorage		Number of anchors
		End U-wraps	CFRP spike anchors	
CB	–	–	–	–
SB.Sh.S	1.0	–	–	–
SB.Sh.F	1.69	–	–	–
SB.Sh.S-U	1.0	✔	✔	2
SB.Sh.S-2A	1.0	–	✔	2
SB.Sh.S-3A	1.0	–	✔	3
SB.Sh.S-4A	1.0	–	✔	4

full-length CFRP laminates covering the entire shear span, while the other specimen was partially strengthened covering 40% of the shear span (1.69 m and 1 m, respectively). One beam was strengthened with CFRP laminate that was anchored with a layer of 200 mm wide end U-wraps. Figure 2 shows the strengthening configuration of specimens SB.Sh.S, SB.Sh.F, and SB.Sh.S-U.

Three RC specimens were strengthened with CFRP laminates anchored with CFRP spike anchors. The length of the CFRP sheets of 1 m and hole diameter of 10 mm for the spike anchor were kept constants for all specimens. In addition, the anchor diameter, anchor embedment depth, and splay length were 8 mm, 40 mm, and 60 mm respectively, for all the beams. The anchor diameter of 8 mm was chosen to fit in the 10 mm diameter hole. The 10 mm diameter hole is typical in this strengthening technique. The 40 mm embedment depth was chosen to be 4 times the hole diameter. The splay length has been taken as 60 mm to establish the required fan angle and cover the sheet width. The variable tested was the number of anchors. In future research, the anchor diameter, anchor depth, and splay length should be varied to study their effects. Figure 3 shows the dimensions and location of the drilled holes for all CFRP anchor configurations. As seen from Fig. 3, all holes were drilled at the center of the laminate width at a distance of 50 mm from both ends of the CFRP laminate.

Table 2 Steel bars mechanical properties

Bar diameter (mm)	f_y (MPa)	ε_y (mm/mm)	f_u (MPa)	E_s (GPa)
8	618 ± 10.7	0.0035 ± 0.0001	683 ± 4.3	193 ± 2
10	621 ± 17.0	0.0041 ± 0.0002	731 ± 15.8	182 ± 8

Table 3 Mechanical properties of CFRP sheet, CFRP laminate, and epoxy adhesive

Material	Density	Thickness (mm)	Tensile strength (MPa)	Elastic modulus (MPa)	Strain at break (%)
CFRP sheet	1.82 g/cm^3	0.167 (dry)	4000	230,000	1.70
CFRP laminate		0.167 (nominal)	3200	210,000	1.59
Epoxy adhesive	1.40 kg/l		30	4.5	0.90

(a) SB.Sh.S

(b) SB.Sh.F

(c) SB.Sh.S-U
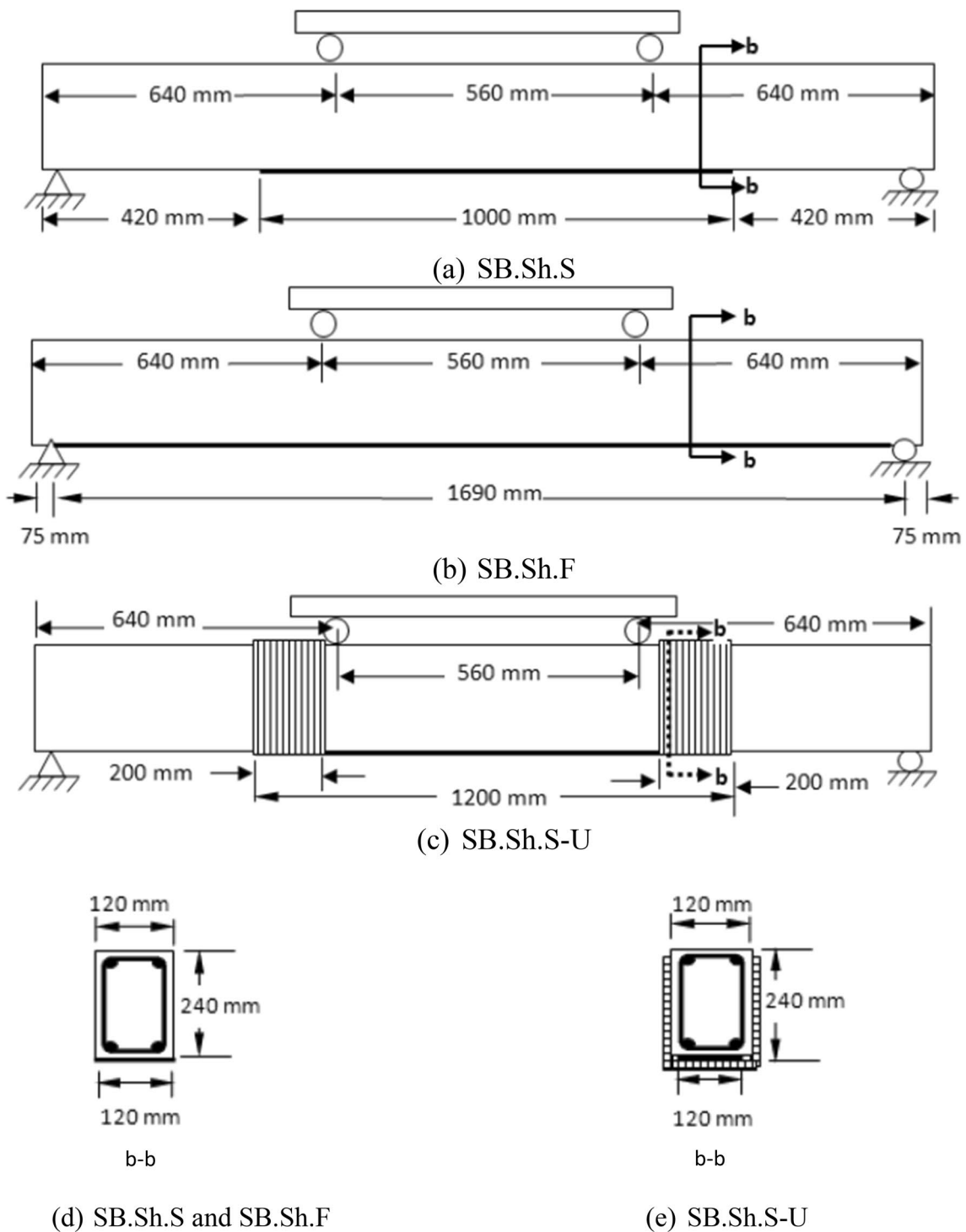
b-b

b-b

(d) SB.Sh.S and SB.Sh.F

(e) SB.Sh.S-U

Fig. 2 Strengthening detailing

3.4 Strengthening procedure

Prior to applying CFRP material, the beams surfaces were conditioned by using a steel-disk mechanical grinder to grind off any uneven spots, as demonstrated in Fig. 4(a).

Holes for the spike anchors were then drilled to the design depth of 40 mm using an electrical drill at pre-specified locations, as shown in Fig. 4(b). The surfaces and the holes were then cleaned from any fine or loose particles using a pressurized air blower. The depth of the holes was

Fig. 3 Bottom view of the specimens showing the dimensions (in mm) and location of the drilled holes for CFRP anchor installation
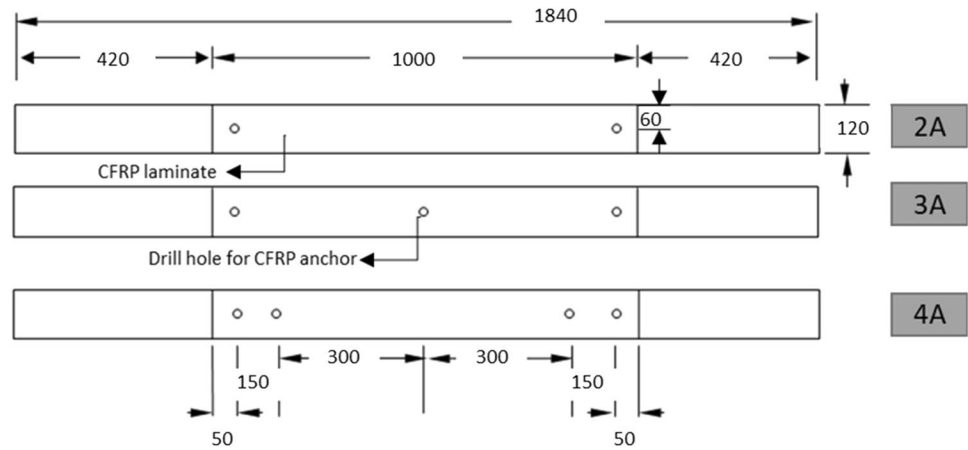
Fig. 4 Strengthening procedure
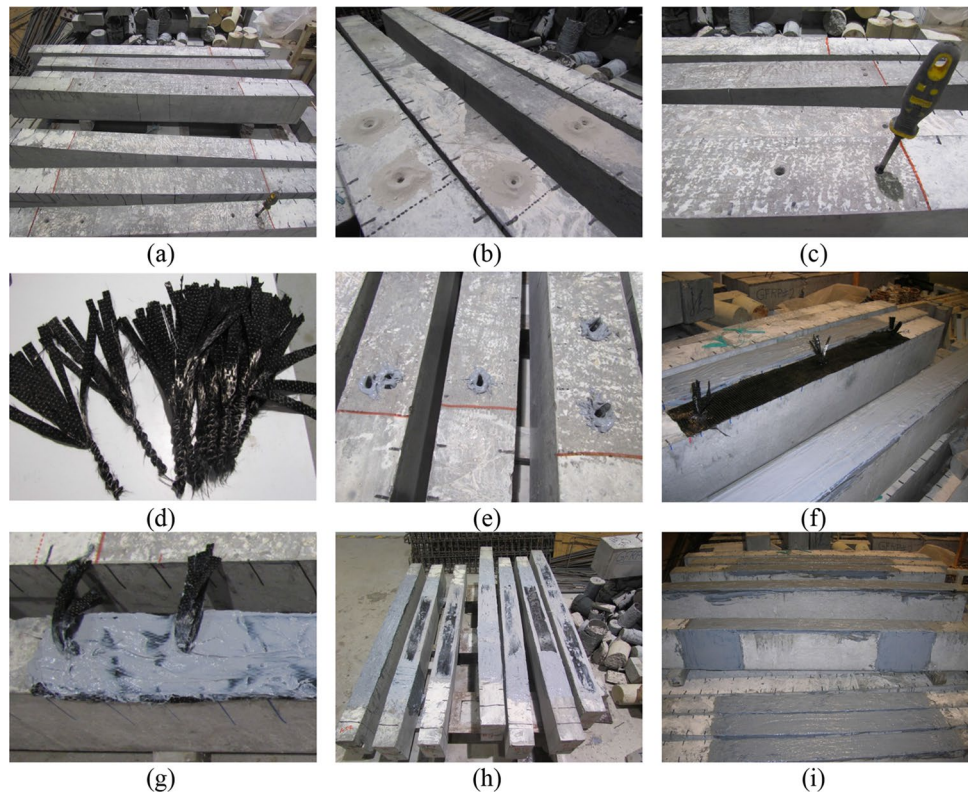
rechecked to ensure it complies with the design of the experiment (Fig. 4(c)).

CFRP unidirectional FRP sheets [47] were cut according to the specified dimensions, and the U-wraps and spike anchors were prepared from the same CFRP material. To prepare the U-wraps, two CFRP sheets of 200 mm wide and 600 mm long were cut. For the 8 mm diameter spike anchors, 50×200 mm CFRP sheets were cut from the CFRP roll. The sheets were then rolled until the 8 mm diameter was attained. The 50×200 mm CFRP sheet was cut further into five 10 mm wide pieces before binding them all together to form the anchor. The anchors were then tied using commercially available mild-steel wire throughout anchor embedment part, as shown in Fig. 4(d). The steel wire was left in place for easier anchor installation. The result was a 200 mm long anchor composed of 40 mm embedment depth and 60 mm splay length.

After preparing the CFRP sheets and anchors, the epoxy resin was mixed in a ratio of 4:1 by weight, as specified by the manufacturer. A layer of the epoxy was then applied onto the concrete surface at the location of the CFRP sheets. For the specimens with spike anchors, the holes were filled approximately half-way with epoxy resin, as displayed in Fig. 4(e). Next, CFRP sheets were placed onto the beams

at their specified locations. Then, the FRP anchors were inserted into the holes by opening the carbon-fiber sheet bundles transversely without damaging or cutting the fibers, as seen in Fig. 4(f). Following that, a low viscosity primer was applied onto the CFRP sheet. After waiting approximately 10 min to allow the saturant to impregnate into the carbon fiber sheet and into the embedded FRP anchors, a second application of epoxy resin layer was applied to the top of the FRP sheet and the splayed FRP anchor fibers. This step was essential to ensure that the two elements are bonded together during curing, as shown in Fig. 4(g). A roller was then used to remove any trapped air and to impregnate the fibers firmly. The prepared specimens are shown in Fig. 4(h). The specimen anchored with end U-wraps was prepared in a similar manner where the epoxy was first applied at the location of CFRP flexural sheets and U-wraps. Then, the CFRP sheet was placed onto the tension side, followed by the U-wraps, and finally, the CFRP was impregnated by an epoxy layer, as shown in Fig. 4(i).

3.5 Test setup and instrumentation

All beam specimens were loaded under four-point bending with a shear span of 565 mm and with the load acting at the mid-span. The load was applied using a universal testing machine (UTM) that has a maximum loading capacity of 1000 kN (dynamic load) and 1200 kN (static load). The tests conducted for all beams were displacement-controlled with a rate of 2 mm/min. Measurement of strains in the external CFRP sheets was taken using electrical resistance strain gauges with gauge lengths of mostly 5 mm. The FRP strain gauges were located at mid-span of the beams. Figure 5 shows the test setup and testing equipment used in this project.
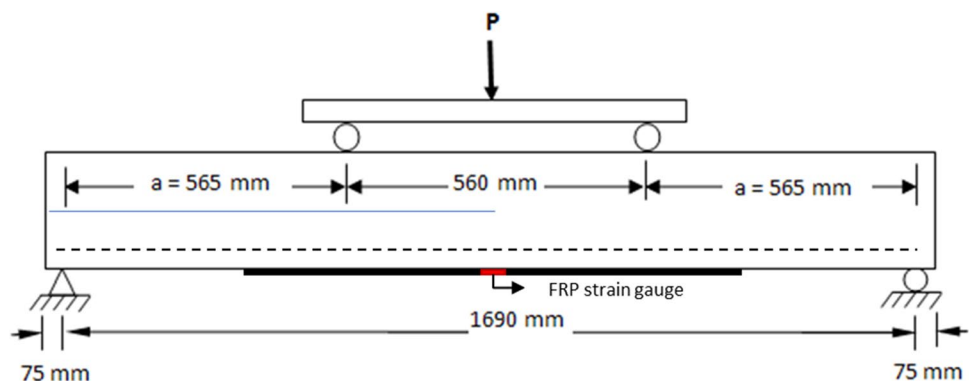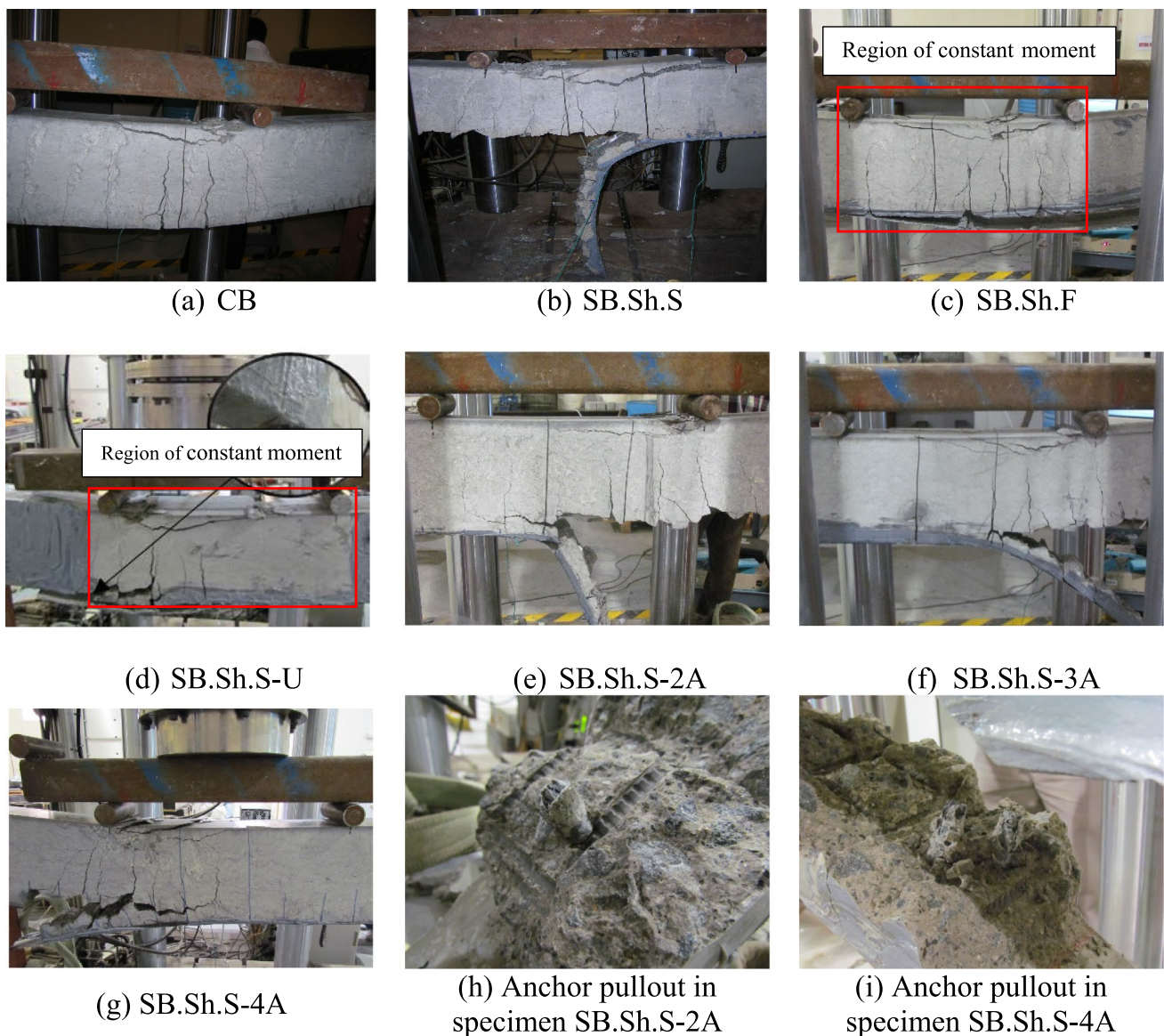
4 Test results

4.1 Failure modes

Figure 6 shows the failure modes of the tested beam specimens. Failure of the control beam (CB) was initiated by vertical flexural cracks that occurred at mid-span (between the two loading points). The crack formation was followed by crushing of concrete at the top compression zone at the vicinity of the beam's mid-span, as shown in Fig. 6(a). The control specimen behaved in a manner corresponding to a typical under-reinforced ductile member.

The strengthened specimens failed in a different manner than the control beam. For SB.Sh.S specimen, the failure was initiated by vertical flexural cracks forming in the middle region. The cracks grew up from tiny unobservable lines to wide thick openings that were easily noticed as the load increased. Failure occurred because of concrete cover separation (around 30 mm thick layer of concrete), which started from one end of the attached sheet and propagated toward the center of the beam. Longitudinal and shear reinforcement were visible after the concrete cover delamination failure. Cracks that caused the failure of the beam were inclined shear-flexural cracks that were initiated at the edges of the attached sheet resulting in concrete cover delamination. In addition, concrete crushing at the top compression zone was observed, as shown in Fig. 6(b).

For SB.Sh.F specimen, the failure happened by means of cracks that spread throughout the length of the beam. The flexural cracks resulted in increased stresses between the CFRP sheet and epoxy causing sudden debonding of the sheet. The debonding initiated at one end of the CFRP laminate and propagated toward the center of the beam, as shown in Fig. 6(c). It should be noted that concrete crushing in the top compression zone occurred simultaneously with the debonding failure. On the other hand, failure of specimen SB.Sh.S-U that was strengthened with CFRP laminate anchored with end U-wraps was initiated by shear-flexural cracks which propagated from the tension flexural zone at

Fig. 5 Test setup and equipment

(a) CB   (b) SB.Sh.S   (c) SB.Sh.F

(d) SB.Sh.S-U   (e) SB.Sh.S-2A   (f) SB.Sh.S-3A

(g) SB.Sh.S-4A   (h) Anchor pullout in specimen SB.Sh.S-2A   (i) Anchor pullout in specimen SB.Sh.S-4A

Fig. 6 Tested beam specimens at failure

an inclination passing through the U-wrapped sheets and ending up in the compression zone of the beam. As the loading was increased, more flexural cracks appeared in other locations between mid-span and the support. Accordingly, the CFRP U-wrapped sheets ruptured under one of the point loads (sheet edge) resulting in an explosive and sudden failure of the specimen and debonding of the CFRP sheet, as shown in Fig. 6(d). Also, concrete crushing at the top compression zone between the two loadings points was visible.

Specimens SB.Sh.S-2A, SB.Sh.S-3A, and SB.Sh.S-4A that were anchored with CFRP spike anchors failed by concrete cover delamination. Flexural-shear cracks started from the bottom tension zone and extended in an inclined mode all through the beam depth till the top compression zone. The higher concentration of the cracks near one edge of the attached sheet resulted in a thick concrete cover separation (around 40 to 60 mm in these beams), as shown in Fig. 6(e–g). The 40 mm depth anchors were pulled out with the thick concrete cover, as displayed in Figs. 6(h) and (i). In addition, concrete crushing was visible in all beams.

Overall, increasing the length of the CFRP sheet (specimen SB.Sh.F) increased the load-carrying capacity of the specimen and changed the mode of failure from concrete cover delamination (specimen SB.Sh.S) to FRP sheet debonding which is less destructive. In addition, even though all anchored specimens failed by concrete cover delamination, the delamination failure was delayed,

and the beams failed at higher loads than the unanchored specimen of the same CFRP length due to the presence of anchors.

4.2 Ultimate load-carrying capacity and load–deflection responses

Table 5 summarizes the test results in terms of the steel yielding load (P_y), deflection at yield (δ_y), ultimate load (P_u), deflection at ultimate load (δ_u), failure load (P_f) calculated as

Table 5 Summary of test results

Specimen	P_y (kN)	δ_y (mm)	P_u (kN)	δ_u (mm)	P_f (kN)	δ_f (mm)	Failure mode
CB	51.7	5.4	68.0	30.3	54.4	45.3	SY, CC
SB.Sh.S	67.1	5.2	79.1	26.0	63.3	33.3	CCD, CC
SB.Sh.F	77.0	6.7	91.2	11.1	72.9	35.7	SD, CC
SB.Sh.S-U	88.7	8.3	95.9	13.2	76.7	41.1	R (U-wraps), SD
SB.Sh.S-2A	75.2	6.3	80.2	7.3	64.1	24.8	CCD, CC
SB.Sh.S-3A	77.5	6.1	83.0	7.7	66.4	24.8	CCD, CC
SB.Sh.S-4A	75.4	6.7	83.2	8.6	66.6	22.2	CCD, CC

SY flexural steel yielding, *CC* concrete crushing, *CCD* concrete cover delamination, *SD* sheet debonding, *R* rupture of the U-wrapped laminates
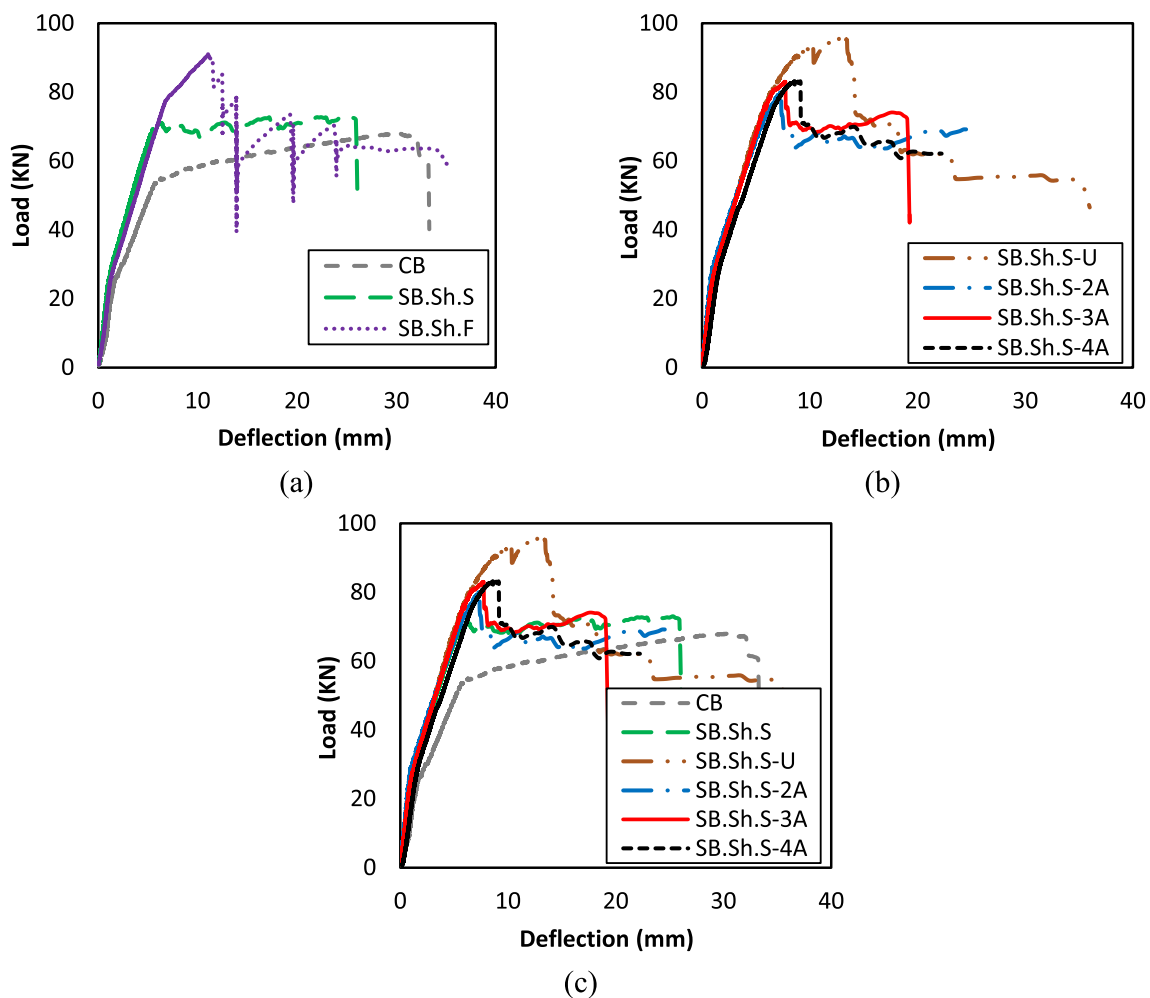
Fig. 7 Load–deflection responses: **a** CB and unanchored specimens; **b** anchored specimens; and **c** CB and all specimens with same CFRP length
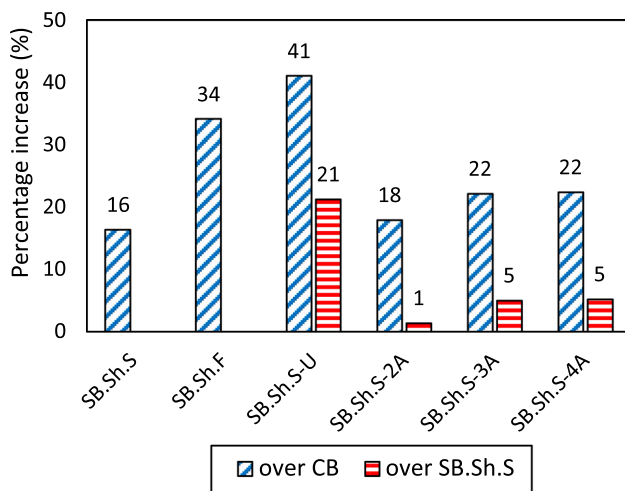
Fig. 8 Percentage increase in P_u over CB and SB.Sh.S

80% of the ultimate load, deflection at failure load (δ_f), and observed failure mode. Figure 7 shows the load–deflection responses of the specimens tested in this study grouped by: (a) control beam and unanchored specimens, (b) anchored specimens, and (c) CB and strengthened specimens with short CFRP length. In addition, the percentage increase values in the ultimate load compared to CB and SB.Sh.S are displayed in bar chart form in Fig. 8.

It is evident from Fig. 7 that the stiffness of the tested specimens was similar before cracking (up to ~25kN). Post-cracking, the stiffness of all specimens decreased due to the development of flexural cracks. The strengthened specimens demonstrated higher stiffness than the control beam (CB) post-cracking, as shown in Fig. 7. In general, results in Fig. 7 and Table 5 show that the strengthened specimens achieved higher loads but lower deflections than the unstrengthened control beam. Particularly, the yield load (P_y) of the strengthened specimens was significantly higher than the control specimen by 30–72%. It was noted that the deflection at yield load (δ_y) was improved in all strengthened beams except SB.Sh.S which experienced a reduction of only 4% in δ_y compared to CB. After the yield point, the stiffness of the tested specimens degraded up to the ultimate state. All strengthened specimens achieved considerably higher ultimate load than CB by 16–41%. The effect of anchorage was evident in enhancing the load-carrying capacity, where the anchored specimens achieved higher loads up to 21% than the strengthened unanchored specimen SB.Sh.S.

Following the ultimate state, there was a drop in the load–deflection curve of specimen CB due to failure. Despite this, specimen CB exhibited the highest deflection of all specimens, which is typical for under reinforced RC beams. On the other hand, the strengthened specimens achieved lower deflections at ultimate and failure loads than CB due to the brittle concrete cover delamination failure.

4.3 Strain analysis

The strain in the external CFRP reinforcement of the strengthened specimens at mid-span was monitored throughout the experiment. Figure 9 provides the load–strain curves for the tested beams. It can be indicated from Fig. 9 that the strain in the CFRP laminates was minimal prior to cracking (~25 kN). After that, the strain values in the CFRP laminates started to increase as the load increased, indicating the contribution of CFRP in carrying the load. The maximum recorded strain values in the unanchored specimens SB.Sh.S and SB.Sh.F were 0.002 and 0.007, respectively. The difference in values is attributed to the length of the FRP; increasing the CFRP length delayed the delamination failure; hence, utilized more strain and enhanced the beam's capacity. Compared to SB.Sh.S, anchoring the CFRP laminates with end U-wraps and CFRP spike anchors delayed delamination failure, thus increasing the strain utilization in the CFRP laminates. Particularly, the maximum CFRP strain attained in the anchored laminates ranged from 0.002 to 0.006 corresponding to 10–34% strain utilization. It should be noted that the maximum strain attained in all beam specimens was lower than the rupture strain of the CFRP proving that none of the beams failed by CFRP rupture.

4.4 Ductility analysis

The ductility indices of the tested beams were calculated using values projected from the load–deflection curves. The ductility was evaluated on a quantitative basis by computing ductility indices in terms of mid-span deflection at ultimate and failure loads to that at yielding of the tension steel. The deflection ductility index at ultimate load
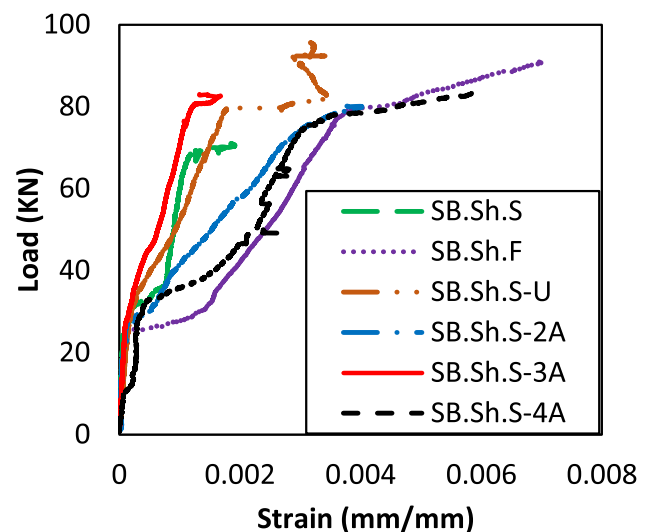
Fig. 9 Load–CFRP strain curves of the strengthened beams

Table 6 Summary of ductility indices

Specimen	$\mu_{\Delta,ult}$	% Decrease over CB	$\mu_{\Delta,fail}$	% Decrease over CB
CB	5.61		8.36	
SB.Sh.S	5.01	11	6.40	24
SB.Sh.F	1.66	70	5.35	36
SB.Sh.S-U	1.60	72	4.97	41
SB.Sh.S-2A	1.17	79	3.94	53
SB.Sh.S-3A	1.25	78	4.04	52
SB.Sh.S-4A	1.29	77	3.34	60
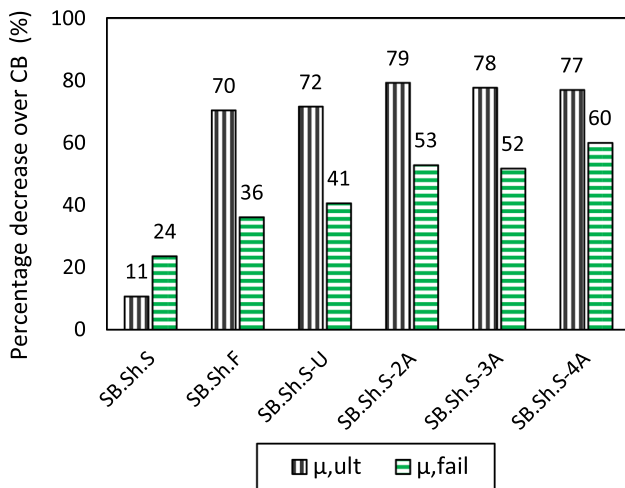
Fig. 10 Percentage decrease in ductility indices over CB

($\mu_{\Delta,ult}$) and the ductility index at failure load ($\mu_{\Delta,fail}$) were computed using the following equations:

$$\mu_{\Delta,ult} = \frac{\delta_u}{\delta_y} \tag{1}$$

$$\mu_{\Delta,fail} = \frac{\delta_f}{\delta_y} \tag{2}$$

Table 6 summarizes the ductility indices calculated at ultimate and failure loads. In addition, the percentage decrease in the ductility over the control specimen (CB) is shown in Table 6 and Fig. 10. It is evident from Table 6 and Fig. 10 that the ductility of all strengthened specimens was inferior to the control specimen (CB). This behavior is attributed to the brittle concrete cover delamination failure. Particularly, the percentage decrease in the ductility over CB at ultimate and failure loads ranged between 11–79% and 24–60%, respectively. Specimen SB.Sh.S that was strengthened with one short-length CFRP laminate

displayed the best ductility performance with only 11 and 24% decrease in $\mu_{\Delta,ult}$ and $\mu_{\Delta,fail}$ than CB, respectively. All other strengthened specimens exhibited very low ductility at ultimate and failure loads.

The anchorage had an adverse effect on the ductility performance of the specimens. Specimen SB.Sh.S-U that was anchored with end U-wraps displayed lower ductile behavior than the unanchored specimen SB.Sh.S by 68 and 22% at ultimate and failure loads, respectively. Similarly, specimens strengthened with CFRP spike anchors showed lower ultimate and failure ductility than SB.Sh.S by 74–77% and 37–48%, respectively. The number of spike anchors did not have any direct effect on the ductility performance of the anchored specimens.

5 Discussion of results

5.1 1Effect of FRP length

This subsection compares the results of specimens SB.Sh.S and SB.Sh.F that were strengthened with 1 m and 1.69 m long CFRP sheets corresponding to 40% and 100% of the beam span, respectively. Test results shown in Table 5 and Figs. 7 and 8 show that increasing the CFRP length had beneficial effects in terms of enhancing the capacity of the beams. Particularly, the yield, ultimate, and failure loads of specimen SB.Sh.F were improved by 15% compared to SB.Sh.S. The increased load-carrying capacity of specimen SB.Sh.F came at the expense of ductility as was discussed in Sect. 4.4. In fact, the ductility at ultimate and failure loads of specimen SB.Sh.F was inferior to that of specimen SB.Sh.S by 67 and 16%, respectively.

The enhancement in the capacity when longer CFRP sheet was used could be attributed to the stress concentration region. The overstressed region and stress concentration at the end of the CFRP laminate are increased when shorter CFRP lengths are used [48]. This results in faster crack initiation and propagation at the end of the CFRP sheet which reduces the capability of the CFRP to withstand more load before failure. Studies in the literature have proven that increasing the ratio of CFRP length to span length increases the capacity of the beams up to a certain point, after which the enhancement becomes marginal [48, 49]. Therefore, it is suggested that more CFRP lengths are investigated in future studies to identify this threshold.

5.2 Effect of anchorage

Two types of anchorage systems were investigated in this study: end U-wraps and CFRP spike anchors. The two types displayed better overall performance compared to the unanchored specimen with similar CFRP length (SB.Sh.S). The

end U-wraps provided the best enhancement in the load-carrying capacity of the beams with 21% increase in P_u compared to SB.Sh.S. This is because the end U-wraps provided confinement to the flexural CFRP sheet at the termination points. This resulted in resisting the tensile peeling stresses and crack propagation at the fiber ends, thus delaying the debonding failure [50]. As a result, more CFRP stress was utilized, and higher capacity was attained. This specimen failed by rupture of one of the U-wraps at the beam's corner which caused debonding in the CFRP sheet at that point. Therefore, the efficiency of this type of anchorage could be improved by using more layers of CFRP U-wraps.

With respect to CFRP spike anchors, the anchors were beneficial in enhancing the yield load by 12–15% compared to the unanchored specimen SB.Sh.S. However, the ultimate capacity of the anchored specimens was only enhanced by 1–5% compared to SB.Sh.S. Increasing the number of anchors increased the ultimate load but in a nonproportional manner. Particularly, anchoring the CFRP laminate with two, three, and four anchors enhanced the ultimate load-carrying capacity by 1.3, 5.0, and 5.2%, respectively. Several reasons caused the deficiency of the CFRP spike anchors as opposed to end U-wraps. First, the embedment depth of the anchors was only 40 mm, which was less than the concrete cover. As a result, the anchors were pulled out with the concrete cover as delamination occurred. The pullout capacity of the anchors could have been improved if longer embedment depths were used [3, 51]. The efficiency of the anchors could have also been enhanced if a larger than 8 mm dowel diameter was used. The diameter and length of the spike anchors must be varied in future research work.

6 Benchmarking using an analytical model

The aim of this paper is to experimentally investigate the effectiveness of CFRP anchors as an alternative to CFRP wraps, if and when wraps are not feasible to install from a constructability point of view. This section is introduced to benchmark the experimental results with the ACI design guidelines to predict the load-carrying capacity of the strengthened and anchored specimens as well as the control specimen.

The nominal flexural strength of the control specimen was calculated using ACI318-19 [52] design guidelines. In addition, the capacity of the strengthened specimens was calculated in accordance with ACI440.2R-17 [53] design guidelines. The nominal flexural strength of FRP-strengthened members is determined based on strain compatibility, internal force equilibrium, and the controlling mode of failure [53]. Equation (3) is used to compute the nominal flexural moment capacity (M_n) of the strengthened members. It should be noted that the reduction factor

(Ψ_f) was set to unity to allow for a reasonable comparison between the predicted nominal flexural capacity and the experimental results:

$$M_n = A_s f_y \left(d - \frac{\beta_1 c}{2} \right) + \Psi_f A_f f_{fe} \left(d_f - \frac{\beta_1 c}{2} \right) \quad (3)$$

where

$$A_f = n t_f w_f \quad (4)$$

$$f_{fe} = E_f \varepsilon_{fe} \quad (5)$$

where A_s is the area of flexural steel reinforcement (mm^2); f_y is the tensile yield strength of the steel bars (MPa); d is the effective depth of the steel reinforcement (mm); β_1 is the ratio of the depth of equivalent rectangular stress block to the depth of the neutral axis; c is the distance from the extreme compression fiber to the neutral axis (mm); n is the number of FRP sheets; t_f is the thickness of FRP sheet (mm); w_f is the width of FRP sheet (mm); Ψ_f is a strength reduction factor; A_f is the area of FRP reinforcement (mm^2); f_{fe} is the effective stress in the FRP (MPa); E_f is the elastic modulus of FRP (MPa); ε_{fe} is the effective strain in the FRP (mm/mm); and d_f is the effective depth of FRP reinforcement (mm).

According to the ACI440.2R-17 [53], the effective strain in the FRP laminates (ε_{fe}) should be limited to the lesser of the debonding strain (ε_{fd}) or 90% of the rupture strain of FRP (ε_{fu}) using Eq. (6):

$$\varepsilon_{fe} \leq \varepsilon_{fd} = 0.41 \sqrt{\frac{f_c'}{n E_f t_f}} \leq 0.9 \varepsilon_{fu} \quad (6)$$

where f_c' is the compressive strength of concrete (MPa).

Another FRP strain state that could govern the design is the strain in the FRP at which the concrete crushes. Therefore, the effective strain in the FRP at ultimate state could be determined using Eq. 7:

$$\varepsilon_{fe} = \varepsilon_{cu} \left(\frac{d_f - c}{c} \right) - \varepsilon_{bi} \leq \varepsilon_{fd} \quad (7)$$

where ε_{cu} is the crushing strain of concrete taken as 0.003, and ε_{bi} is the initial substrate strain taken as zero.

To calculate the flexural moment capacity of FRP strengthened members, the depth of the neutral axis (c) should be assumed, and then, the strain and the corresponding stress in the concrete, steel, and FRP are calculated based on strain compatibility. The internal force equilibrium should be satisfied; otherwise, the depth of the neutral axis should be reassumed until internal force resultants equilibrate.

Table 7 Analytical predictions using ACI440.2R-17

Specimen	ε_{fe}(mm/mm)	$P_{u,exp}$(kN)	$P_{u,pred}$(kN)	$\frac{P_{u,exp}}{P_{u,pred}}$
CB	–	68.0	66.0	1.03
SB.Sh.S	0.01282	79.1	100.2	0.79
SB.Sh.F	0.01282	91.2	100.2	0.91
SB.Sh.S-U	0.01282	95.9	100.2	0.96
SB.Sh.S-2A	0.01282	80.2	100.2	0.80
SB.Sh.S-3A	0.01282	83.0	100.2	0.83
SB.Sh.S-4A	0.01282	83.2	100.2	0.83

Table 7 summarizes the results in terms of calculated effective strain in CFRP laminates (ε_{fe}), experimental ultimate load ($P_{u,exp}$), predicted ultimate load ($P_{u,pred}$), and ratio of $P_{u,exp}$ to $P_{u,pred}$. It can be depicted from Table 7 that the ACI318-19 [52] design provisions closely predict the capacity of the control specimen with $P_{u,exp}/P_{u,pred} = 1.03$. With respect to the strengthened specimens, the predicted values correspond reasonably well with the experimental values. In particular, the percentage difference between the predicted and tested values ranges from 3 to 23% indicating good agreement with the test results. However, the predictions of the ACI440.2R-17 [53] were slightly unconservative and overestimated for all specimens, especially specimen SB.Sh.S that was strengthened with unanchored short-length CFRP sheet ($P_{u,exp}/P_{u,pred} = 0.79$). In contrast, the ultimate capacity of specimen SB.Sh.F with full-length CFRP sheet was reasonably predicted with $P_{u,exp}/P_{u,pred}$ close to 1. It should be noted that the ACI440.2R-17 [53] design guidelines does not account for variations in the CFRP length. As a result, the analytical predictions obtained for both specimens SB.Sh.S and SB.Sh.F were similar, while in fact, the short-length CFRP sheet provided lower strength enhancement than the full-length CFRP sheet. Hence, the predicted value for specimen SB.Sh.S was unsafe and slightly overestimated the experimental values.

It is clear from Table 7 that the calculated effective strain in the laminates was similar for all strengthened specimens (unanchored and anchored). This is because the predicted effective strain in the laminates was limited by the strain at the limit of concrete crushing. The predicted capacity of the anchored specimens was higher than the experimental values with $P_{u,exp}/P_{u,pred}$ ranged from 0.80 for the specimen with 2 spike anchors to 0.96 for the specimen with side U-wraps.

7 Conclusions

This paper focused on investigating the flexural performance of RC beams strengthened with CFRP laminates. The test parameters included in this study are the length of the CFRP sheet, anchorage type (end U-wraps and CFRP spike anchors), and number of CFRP spike anchors. A total of six strengthened RC beam specimens were tested under four-point bending, and the results were compared with that of a control beam. Based on the analysis of the experimental results, the following conclusions were made:

1. Strengthening of RC beams with CFRP laminates, regardless of the CFRP length and anchorage, enhanced the ultimate load-carrying capacity of the beams by 16–41% compared to the control beam.
2. The beam strengthened with full-length CFRP sheet exhibited higher capacity than that strengthened with short-length CFRP sheet. Particularly, the yield, ultimate, and failure loads of specimen SB.Sh.F were improved by 15% compared to SB.Sh.S.
3. Anchoring the CFRP laminates had beneficial effects in terms of enhancing the overall performance of the beams compared to the unanchored specimen with similar CFRP length (SB.Sh.S). The end U-wraps provided the best enhancement in the load-carrying capacity of the beams with 21% increase in P_u compared to SB.Sh.S.
4. Increasing the number of CFRP spike anchors increased the ultimate load but in a nonproportional manner. Particularly, anchoring the CFRP laminate with two, three, and four anchors enhanced the ultimate load-carrying capacity by 1.3, 5.0, and 5.2%, respectively. The efficiency of the anchors could be improved by using longer embedment depth and larger diameter dowels.
5. All strengthened specimens exhibited lower ductility at ultimate and failure loads than the control beam due to the brittle concrete cover delamination failure.
6. The predictions of flexural strength calculated using the ACI440.2R-17 design guidelines correspond reasonably well with the experimental values but are slightly unconservative. The difference between the experimental and test results ranged between 3 and 23%, indicating good agreement.

Declarations

Conflict of interest The authors declare that they have no known competing financial interests or personal relationships that could have appeared to influence the work reported in this paper.

Ethical approval This article does not contain any studies with human participants or animals performed by any of the authors.

References

1. Dong J, Wang Q, Guan Z. Composites : part B structural behaviour of RC beams with external flexural and flexural—shear strengthening by FRP sheets. Compos B. 2013;44(1):604–12.
2. Amran YHM, Alyousef R, Rashid RSM, Alabduljabbar H. Properties and applications of FRP in strengthening RC structures: a review. Structures. 2018;16:208–38.
3. Mhanna HH, Hawileh RA, Abdalla JA, Salama ASD, Alkhrdaji T. Shear strengthening of reinforced Concrete T-beams with anchored CFRP laminates. J Compos Constr. 2021;25(4):04021030.
4. Helal K, Yehia S, Hawileh R, Abdalla J. Performance of preloaded CFRP-strengthened fiber reinforced concrete beams. Compos Struct. 2020;244: 112262.
5. Godat A, Hammad F, Chaallal O. State-of-the-art review of anchored FRP shear-strengthened RC beams : A Study of Influencing Factors. Compos Struct. 2020;254(June): 112767.
6. Naser MZ, Hawileh RA, Abdalla JA. Fiber-reinforced polymer composites in strengthening reinforced concrete structures: a critical review. Eng Struct. 2019;198: 109542.
7. Nawaz W, Hawileh RA, Saqan EI, Abdalla JA. Effect of longitudinal carbon fiber-reinforced polymer plates on shear strength of reinforced concrete beams. ACI Struct J. 2016;113(3):577–86.
8. Abdalla JA, Hawileh R, Al-tamimi A. Prediction of frp-concrete ultimate bond strength using artificial. https://doi.org/10.1109/ICMSAO.2011.5775518
9. Salama ASD, Hawileh RA, Abdalla JA. Performance of externally strengthened RC beams with side-bonded CFRP sheets. Compos Struct. 2019;212:281–90.
10. Gao R, Cao Q, Hu F, Gao Z, Li F. Experimental study on flexural performance of reinforced concrete beams subjected to different plate strengthening. Compos Struct. 2017;176:565–81.
11. Mhanna HH, Hawileh RA, Abdalla JA. Shear behavior of RC T-beams externally strengthened with anchored high modulus carbon fiber-reinforced polymer (CFRP) laminates. Compos Struct. 2021;272: 114198.
12. Ozden S, Atalay HM, Akpinar E, Erdogan H, Vulaş YZ. Shear strengthening of reinforced concrete T-beams with fully or partially bonded fibre-reinforced polymer composites. Struct Concr. 2014;15(2):229–39.
13. Dai JG, Lam L, Ueda T. Seismic retrofit of square RC columns with polyethylene terephthalate (PET) fibre reinforced polymer composites. Constr Build Mater. 2012;27(1):206–17.
14. Yan L, Chouw N. Natural FRP tube confined fibre reinforced concrete under pure axial compression: a comparison with glass/carbon FRP. Thin-Walled Structures. 2014;82:159–69.
15. Popescu C, Schmidt JW, Goltermann P, Sas G. Assessment of RC walls with cut-out openings strengthened by FRP composites using a rigid-plastic approach. Eng Struct. 2017;150:585–98.
16. Mutalib AA, Hao H. The effect of anchorages on FRP strengthening of RC walls to resist blast loads. Appl Mech Mater. 2011;82:497–502.
17. Tahsiri H, Sedehi O, Khaloo A, Raisi EM. Experimental study of RC jacketed and CFRP strengthened RC beams. Constr Build Mater. 2015;95:476–85.
18. Li S, Wang XG, Zhou XG. Debonding behaviors of CFRP strengthened RC beams with weak interfaces. Appl Mech Mater. 2013;351–352:587–91.
19. Ceroni F, Pecce M, Matthys S, Taerwe L. Debonding strength and anchorage devices for reinforced concrete elements strengthened with FRP sheets. Compos B Eng. 2008;39:429–41.
20. Chen GM, Teng JG, Chen JF. Process of debonding in RC beams shear-strengthened with FRP U-strips or side strips. Int J Solids Struct. 2012;49(10):1266–82.
21. Saqan EI, Rasheed HA, Alkhrdaji T. Seismic behavior of carbon fiber-reinforced polymer- strengthened reinforced concrete members with various anchors. ACI Struct J. 2020;117(4):3–14.
22. Baggio D, Soudki K, Noël M. Strengthening of shear critical RC beams with various FRP systems. Constr Build Mater. 2014;66:634–44.
23. Bae S, Belarbi A. Behavior of various anchorage systems used for shear strengthening of concrete structures with externally bonded FRP sheets. J Bridg Eng. 2013;18:837–47.
24. del Rey CE, Dizhur D, Griffith M, Ingham J. Strengthening RC structures using FRP spike anchors in combination with EBR systems. Compos Struct. 2019;209:668–85.
25. Wang X, Pan JW, Xia JF, Wu F. Study on hybrid effects of FRP anchors for strengthening of concrete structures. IOP Conf Ser Mater Sci Eng. 2018;422(1):012013.
26. Sun W, Liu S, Zhang C. An effective improvement for enhancing the strength and feasibility of FRP spike anchors. Compos Struct. 2020;247: 112449.
27. Gora AM, Jaganathan J, Anwar MP, Leung HY. Flexural capacity of bi-directional GFRP strengthened RC beams with end anchorages. Int J Struct Integr. 2018;188:188–207.
28. Valivonis J, Skuturna T, Valivonis J, Skuturna T. Cracking and strength of reinforced concrete structures in flexure strengthened with carbon fibre laminates. 2010; 3730.
29. Haddad RH, Marji CS. Composite strips with U-shaped CFRP wrap anchor systems for strengthening reinforced concrete beams. Int J Civ Eng. 2019;17(11):1799–811.
30. Saqan EI, Rasheed HA, Hawileh RA. An efficient design procedure for flexural strengthening of RC beams based on ACI 440.2R–08. Compos Part B Eng. 2013;49:71–9.
31. Al-Tamimi AK, Hawileh R, Abdalla J, Rasheed HA. Effects of ratio of CFRP plate length to shear span and end anchorage on flexural behavior of SCC RC beams. J Compos Constr. 2011;15(6):908–19.
32. Zhang Y, Nehdi ML. Experimental and analytical investigation on flexural retrofitting of RC T-section beams using CFRP sheets. Appl Sci. 2020;10:1233.
33. Zaki MA, Rasheed HA. Behavior of reinforced concrete beams strengthened using CFRP sheets with innovative anchorage devices. Eng Struct. 2020;215: 110689.
34. Eshwar N, Nanni A, Ibell TJ. Performance of two anchor systems of externally bonded fiber-reinforced polymer laminates. ACI Mater J. 2008;105:72–81.
35. Al-Atta B, Kalfat R, Al-Mahaidi R, Al-Mosawe A. Influence of anchorage systems on externally-bonded CFRP sheets used for flexural strengthening. Int Conf Eng Sci. 2020;671:012105.
36. Lim J, Kim J, del Rey Castillo E, Griffith MC, Dizhur D, Ingham JM. Characterization of Bent Fibre Reinforced Polymer (FRP) Anchors Exhibiting Fibre Rupture Failure Mode. Proceedings of The New Zealand Concrete Industry Conference 2016; (October).
37. Kalfat R. Improvement of FRP-to-concrete bond performance using bidirectional fiber patch anchors combined with FRP spike anchors. Compos Struct. 2016;155:89–98.

38. Kalfat R, Al-Mahaidi R. Mitigation of premature failure of FRP bonded to concrete using mechanical substrate strengthening and FRP spike anchors. Compos B. 2016;94:209–17.

39. Kim SJ, Smith ST. Behaviour of handmade FRP anchors under tensile load in uncracked concrete. Adv Struct Eng. 2009;12(6):845–66.

40. Zaki MA, Rasheed HA, Roukerd RR, Raheem M. Performance of reinforced concrete T beams strengthened with flexural CFRP sheets and secured using CFRP splay anchors. Eng Struct. 2020;210: 110304.

41. Kim I, Jirsa JO, Bayrak O. Anchorage of carbon fiber-reinforced polymer on side faces of reinforced concrete beams to provide continuity. ACI Struct J. 2013. https://doi.org/10.14359/51686163.

42. ASTM C39/C39M-18. Standard Test Method for Compressive Strength of Cylindrical Concrete Specimens. ASTM International, West Conshohocken, PA; 2018.

43. ASTM C496/C496M-11. Standard Test Method for Splitting Tensile Strength of Cylindrical Concrete Specimens. ASTM International, West Conshohocken, PA; 2017. .

44. BS 1881–116. BS 1881–116:1983. Testing Concrete. Part 116: Method for determination of compressive strength of concrete cubes. British Standard Institution, London, UK; 2019. British Standards Institution (BSI) 1983;

45. SikaWrap-300C. Woven Unidirectional Carbon Fibre Fabric, designed for Structural Strengthening Applications as Part of the SIKA Strengthening System. Product data sheet from Sika; Sika GCC, UAE; 2017.

46. Sikadur-330. Two-part epoxy impregnation resin. Product data sheet from Sika; Sika GCC, UAE; 2017.

47. SikaWrap-300C. Carbon fiber fabric for structural strengthening. product data sheet from Sika; Sika Schweiz AG, Zürich, Switzerland.2003;1–3.

48. Ding J, Wang F, Huang X, Chen S. The effect of CFRP length on the failure mode of strengthened concrete beams. Polymers. 2014;6:1705–26.

49. Mohammed M, Kadhim A. Effect of CFRP plate length strengthening continuous steel beam. Constr Build Mater. 2012;28(1):648–52.

50. Kalfat R, Al-Mahaidi R, Scott T. Anchorage devices used to improve the performance of reinforced concrete beams retrofitted with FRP composites : State-of-the-Art review. J Compos Constr. 2013;17(1):14–33.

51. del Rey CE, Kanitkar R, Smith ST, Gri MC, Ingham JM. Design approach for FRP spike anchors in FRP-strengthened RC structures. Compos Struct. 2019;214:23–33.

52. Bai Y, Dai J, Mohammadi M, Lin G, Mei S. Stiffness-based design-oriented compressive stress-strain model for large-rupture-strain (LRS) FRP-confined concrete. Compos Struct. 2019;223: 110953.

53. ACI440.2R-17. Guide for the Design and Construction of Externally Bonded FRP Systems for Strengthening Concrete Structures. American Concrete Institute, Farmington Hills, U.S.A.2017;